

New Weighted Taylor Series for Water Wave Energy Loss and Littoral Current Analysis

Syawaluddin Hutahaean

Ocean Engineering Program, Faculty of Civil and Environmental Engineering-Bandung Institute of Technology (ITB), Bandung 40132, Indonesia.

syawalf1@yahoo.co.id

Received: 15 Dec 2024,

Receive in revised form: 13 Jan 2025,

Accepted: 19 Jan 2025,

Available online: 25 Jan 2025

©2025 The Author(s). Published by AI
Publication. This is an open-access article under
the CC BY license

(<https://creativecommons.org/licenses/by/4.0/>).

Keywords— *weighted Taylor series, weighting coefficients, littoral current.*

Abstract—*This paper presents a more systematic formulation of the weighted Taylor series, resulting in a more accurate determination of the weighting coefficient. The weighted Taylor series is derived by truncating the Taylor series to the first order and assigning weighting coefficients to the first-order terms, which reflect the contribution of higher-order terms. The resulting weighted Taylor series is applied to the analysis of wave constant equations in deep water, including wavelength and wave period, which are primarily governed by the Kinematic Free Surface Boundary Condition. The input for these wave constant equations is the wave amplitude. Using these wave constant equations, a shoaling-breaking model is developed, accounting for wave energy loss. The lost wave energy is then utilized to derive the radiation current equation, which subsequently leads to the formulation of the littoral current equation.*

I. INTRODUCTION

The fundamental equations of hydrodynamics are often formulated using truncated Taylor series, which retain only the first-order terms. The justification for truncation lies in the assumption that, for sufficiently small intervals in both time and space, the contributions of second-order and higher-order terms become negligible. However, this reasoning is not entirely accurate. As the interval size decreases, the value of the first-order term also diminishes, rendering the higher-order terms relatively significant. Consequently, neglecting these terms can lead to a loss of important characteristics of the underlying function, as higher-order differentials carry specific physical meanings. For instance, second-order differentials are associated with identifying maxima or minima, while third-order differentials convey additional information about the curvature and behavior of the function. Excluding these terms compromises the accuracy and completeness of the representation, as the first-order approximation alone is insufficient to capture the essential properties of the system.

Despite this limitation, incorporating higher-order terms into the formulation of the basic equations of hydrodynamics poses considerable challenges, particularly in terms of complexity and computational feasibility. To address this issue, it is necessary to develop a modified truncated Taylor series that retains the influence of higher-order terms indirectly. This research introduces such a formulation, termed the weighted Taylor series, in which the effects of higher-order terms are embedded into the first-order term through the use of weighting coefficients.

The accurate determination of these weighting coefficients requires careful consideration of the interval size at which the Taylor series can be truncated to a first-order approximation. Consequently, this research also formulates an appropriate interval size for numerical modeling, ensuring that the weighted Taylor series captures the essential dynamics of the system while remaining computationally efficient.

Numerical methods, such as the Finite Difference Method (FDM) and the Finite Element Method (FEM), are

commonly used to solve the governing equations of hydrodynamics. These methods rely on small interval sizes, which must align with the formulation of the basic equations. By integrating the weighted Taylor series and its associated interval size, this research aims to enhance the accuracy and reliability of numerical hydrodynamic models.

An application of these principles can be seen in the research of wave energy dissipation in coastal waters, a phenomenon first described by Longuet-Higgins (1970) as radiation stress. From the radiation stress equations, the longshore current equations were subsequently derived. Understanding longshore currents is crucial, as these currents play a significant role in coastal erosion and sedimentation processes.

II. THE FORMULATION OF WEIGHTED TAYLOR SERIES 2-D

The following is Taylor series for a function with two variables $f = f(x, t)$, (Arden, Bruce W. and Astill Kenneth N., 1970)

$$f(x + \delta x, t + \delta t) = f(x, t) + \delta t \frac{\partial f}{\partial t} + \delta x \frac{\partial f}{\partial x} + \frac{\delta t^2}{2!} \frac{\partial^2 f}{\partial t^2} + \delta t \delta x \frac{\partial^2 f}{\partial t \partial x} + \frac{\delta x^2}{2!} \frac{\partial^2 f}{\partial x^2} + \dots \quad (1)$$

x is the horizontal axis and t is time. The simplified formula is written as follows.

$$f(x + \delta x, t + \delta t) = f(x, t) + s_1 + s_2 + s_3 + \dots + s_n \quad \dots (2)$$

Where,

$$s_1 = \delta t \frac{\partial f}{\partial t} + \delta x \frac{\partial f}{\partial x}$$

$$s_2 = \frac{\delta t^2}{2!} \frac{\partial^2 f}{\partial t^2} + \delta t \delta x \frac{\partial^2 f}{\partial t \partial x} + \frac{\delta x^2}{2!} \frac{\partial^2 f}{\partial x^2}$$

$$s_3 = \frac{\delta t^3}{6} \frac{\partial^3 f}{\partial t^3} + \frac{\delta t^2}{2} \delta x \frac{\partial^3 f}{\partial t^2 \partial x} + \delta t \frac{\delta x^2}{2} \frac{\partial^3 f}{\partial t \partial x^2} + \frac{\delta x^3}{6} \frac{\partial^3 f}{\partial x^3}$$

Etc.

Odd differential terms of higher order are collected,

$$f(x + \delta x, t + \delta t) = f(x, t) + s_1 + s_2 + s_4 + s_6 \dots + \sum_{j=2i+1}^{2n+1} s_j \quad \dots (3)$$

Where $i = 1$ to n . For,

$$\sum_{j=2i+1}^{2n+1} s_j = \mu_2 s_1 \quad \dots \dots (4)$$

The term μ_2 , known as the contribution coefficient, is a small number. Substituting this into (3) yields:

$$f(x + \delta x, t + \delta t) = f(x, t) + (1 + \mu_2)s_1 + s_2 + s_4 + s_6 \dots \quad (5)$$

Expansion to point $(x - \delta x, t - \delta t)$,

$$f(x - \delta x, t - \delta t) = f(x, t) - (1 + \mu_2)s_1 + s_2 + s_4 + s_6 \dots \dots (6)$$

Equation (5) subtracted by equation (6),

$$f(x + \delta x, t + \delta t) - f(x - \delta x, t - \delta t) = 2(1 + \mu_2)s_1$$

s_1 is broken down into,

$$f(x + \delta x, t + \delta t) - f(x - \delta x, t - \delta t) = 2(1 + \mu_2)\delta t \frac{\partial f}{\partial t} + 2(1 + \mu_2)\delta x \frac{\partial f}{\partial x}$$

This equation represents the total change in the function's value as it transitions from $(x - \delta x, t - \delta t)$ ke $(x + \delta x, t + \delta t)$. Subsequently, the equation is normalized by dividing it by $2\delta x$,

$$\frac{f(x + \delta x, t + \delta t) - f(x - \delta x, t - \delta t)}{2\delta x} = (1 + \mu_2) \frac{\partial f}{\partial t} + (1 + \mu_2) \frac{\partial f}{\partial x}$$

At small δx and δt , this equation represents the total change per unit length, specifically:

$$\frac{Df}{dx} = (1 + \mu_2) \frac{\delta t}{\delta x} \frac{\partial f}{\partial t} + (1 + \mu_2) \frac{\partial f}{\partial x} \dots \dots (7)$$

This equation includes higher-order terms, comprising both even and odd differentials. The Taylor series expansion is truncated to the first-order terms only.

$$f(x + \delta x, t + \delta t) = f(x, t) + \delta t \frac{\partial f}{\partial t} + \delta x \frac{\partial f}{\partial x}$$

$\frac{\partial f}{\partial x}$ in the 3rd term on the right side is substituted with (7)

$$f(x + \delta x, t + \delta t) = f(x, t) + \delta t \frac{\partial f}{\partial t} + \delta x \left((1 + \mu_2) \frac{\delta t}{\delta x} \frac{\partial f}{\partial t} + (1 + \mu_2) \frac{\partial f}{\partial x} \right)$$

Similar terms are grouped,

$$f(x + \delta x, t + \delta t) = f(x, t) + (2 + \mu_2)\delta t \frac{\partial f}{\partial t} + (1 + \mu_2)\delta x \frac{\partial f}{\partial x}$$

And later are defined as,

$$\gamma_{t,2} = 2 + \mu_2 \quad \dots \dots (8)$$

$$\gamma_{x,2} = 1 + \mu_2 \quad \dots \dots (9)$$

Hence, the final equation is,

$$f(x + \delta x, t + \delta t) = f(x, t) + \gamma_{t,2}\delta t \frac{\partial f}{\partial t} + \gamma_{x,2}\delta x \frac{\partial f}{\partial x} \quad \dots \dots (10)$$

This equation represents a weighted Taylor series expansion for the function $f = f(x, t)$ and weighting coefficient $\gamma_{t,2}$ and $\gamma_{x,2}$.

a. Calculating the contributing coefficient μ_2 .

Equation (4) can be reformulated to express the contribution coefficient μ_2 , that is

$$\mu_2 = \frac{\sum_{j=2i+1}^{2n+1} S_j}{s_1}$$

For very small interval between δt and δx , thus $(s_5 + s_7 + s_9 + \dots) \ll s_3$. Therefore, the final equation can be approached by,

$$\mu_2 = \frac{s_3}{s_1}$$

s_3 and s_1 are broken down into,

$$\mu_2 = \frac{\frac{\delta t^3}{6} \frac{\partial^3 f}{\partial t^3} + \frac{\delta t^2}{2} \delta x \frac{\partial^3 f}{\partial t^2 \partial x} + \delta t \frac{\delta x^2}{2} \frac{\partial^3 f}{\partial t \partial x^2} + \frac{\delta x^3}{6} \frac{\partial^3 f}{\partial x^3}}{\left(\delta t \frac{\partial f}{\partial t} + \delta x \frac{\partial f}{\partial x} \right)} \dots(11)$$

The sinusoidal water wave equation can apply this formula, $f(x, t) = \cos \sigma t \cos kx$

Where $\sigma = \frac{2\pi}{T}$ and $k = \frac{2\pi}{L}$ where T is wave period and L is wavelength.

The substitution of $f(x, t)$ to (11) within $\cos \sigma t = \sin \sigma t$ and $\cos kx = \sin kx$ is as follows.

$$\mu_2 = \frac{\frac{\delta t^3}{6} \sigma^3 + \frac{\delta t^2}{2} \delta x k \sigma^2 + \delta t \frac{\delta x^2}{2} \sigma k^2 + \frac{\delta x^3}{6} k^3}{(-\delta t \sigma - \delta x k)}$$

The substitution of $\delta t = \varepsilon_t T$, $\sigma = \frac{2\pi}{T}$, $\delta x = \varepsilon_x L$ and $k = \frac{2\pi}{L}$, where ε_t is the interval coefficient of t axis, while ε_x is the interval coefficient of x horizontal axis, thus

$$\mu_2 = \frac{\frac{\varepsilon_t^3}{6} (2\pi)^2 + \frac{\varepsilon_t^2}{2} (2\pi)^2 \varepsilon_x + \varepsilon_t \frac{\varepsilon_x^2}{2} (2\pi)^2 + \frac{\varepsilon_x^3}{6} (2\pi)^2}{(-\varepsilon_t - \varepsilon_x)} \dots(12)$$

This equation is used to calculate the contribution coefficient μ_2 . It involves the time interval coefficient ε_t and interval coefficient $-x$, ε_x , explained as follows.

b. Calculation of Interval Coefficients ε_t and ε_x

In the formulation of the μ_2 contribution equation, it is essential to assume very small intervals δt and δx such that the sum $(s_5 + s_7 + s_9 + \dots) \ll s_3$. This condition necessitates that both δt and δx be sufficiently small.

At very small values of δt and δx , where $s_3 \ll s_2$, the grid size can be determined using the optimization equation:

$$\left| \frac{s_2}{s_1} \right| < \varepsilon$$

ε represents a small positive number known as the optimization coefficient. The terms s_1 and s_2 are further broken down:

$$\left| \frac{\frac{\delta t^2}{2!} \frac{\partial^2 f}{\partial t^2} + \delta t \delta x \frac{\partial^2 f}{\partial t \partial x} + \frac{\delta x^2}{2!} \frac{\partial^2 f}{\partial x^2}}{\delta t \frac{\partial f}{\partial t} + \delta x \frac{\partial f}{\partial x}} \right| < \varepsilon \dots(13)$$

a. Equation for Grid Coefficient ε_t .

To derive the equation for the grid coefficient ε_t , function $f(t)$ is used

$$f(t) = \cos \sigma t$$

Substituting this function into the equation (13) yields:

$$\left| \frac{\frac{\delta t^2}{2!} \frac{\partial^2 f}{\partial t^2}}{\delta t \frac{\partial f}{\partial t}} \right| < \varepsilon$$

Substituting $f(t)$ and applying the condition $\cos \sigma t = \sin \sigma t$, we remove the absolute value sign and simplify the expression to:

$$\frac{\delta t}{2} \sigma = \varepsilon$$

Substituting $\delta t = \varepsilon_t T$ and $\sigma = \frac{2\pi}{T}$, yields the following equation

$$\varepsilon_t = \frac{\varepsilon}{\pi} \dots(14)$$

This equation is used to calculate the grid coefficient ε_t .

b. Equation for Grid Coefficient ε_x .

The following equation is used

$$f(x, t) = \cos \sigma t \cos kx$$

Substituting $f(x, t)$ into (13) under the condition $\cos \sigma t = \sin \sigma t$ and $\cos kx = \sin kx$ is

$$\left| \frac{-\frac{\delta t^2}{2} \sigma^2 + \delta t \delta x k \sigma - \frac{\delta x^2}{2} k^2}{-\delta t \sigma - \delta x k} \right| \leq \varepsilon$$

Multiplying both the numerator and denominator by -1

$$\left| \frac{\frac{\delta t^2}{2} \sigma^2 - \delta t \delta x k \sigma + \frac{\delta x^2}{2} k^2}{\delta t \sigma + \delta x k} \right| \leq \varepsilon$$

Since the expression within the absolute value sign must be positive, the absolute value sign can be removed and multiply the denominator on the right-hand side of the equation.

$$\frac{\delta t^2}{2} \sigma^2 - \delta t \delta x k \sigma + \frac{\delta x^2}{2} k^2 \leq \varepsilon (\delta t \sigma + \delta x k)$$

Substituting $\delta t = \varepsilon_t T$, $\delta t = \varepsilon_x L$, $\sigma = \frac{2\pi}{T}$ and $k = \frac{2\pi}{L}$, and assuming equality, we move the right-hand side to the left-hand side:

$$\frac{\varepsilon_x^2}{2} - \left(\varepsilon_t + \frac{\varepsilon}{2\pi} \right) \varepsilon_x + \frac{\varepsilon_t^2}{2} - \frac{\varepsilon \varepsilon_t}{2\pi} = 0 \quad \dots (15)$$

In this equation, ε_t is already known from equation (14). There are two possible values for ε_x , and the larger of the two is selected.

Table (1) Results of ε_t and ε_x calculation

ε	ε_t	ε_x	$\frac{\varepsilon_x}{\varepsilon_t}$
0.01	0.003183	0.009549	3.000000
0.02	0.006366	0.019099	3.000000
0.03	0.009549	0.028648	3.000000
0.04	0.012732	0.038197	3.000000
0.05	0.015915	0.047746	3.000000
0.06	0.019099	0.057296	3.000000
0.07	0.022282	0.066845	3.000000
0.08	0.025465	0.076394	3.000000
0.09	0.028648	0.085944	3.000000
0.10	0.031831	0.095493	3.000000

The calculation results for the grid coefficients presented in Table (1) reveal that as the optimization coefficient ε increases, both grid coefficients ε_t and ε_x also increase, which is expected. Of particular interest is the ratio $\frac{\varepsilon_x}{\varepsilon_t}$ of 3.0.

From the definition,

$$\frac{\varepsilon_x}{\varepsilon_t} = \frac{\delta x}{L} \frac{1}{\delta t/T} = \frac{\delta x T}{\delta t L}$$

$$\frac{\delta x T}{\delta t L} = 3.0$$

$$\frac{\delta x}{\delta t} = 3.0 \frac{L}{T}$$

$\frac{L}{T}$ is wave celerity C , thus

$$\frac{\delta x}{\delta t} = 3.0 C$$

This equation is consistent with the Courant (1928) criterion.

Table (2): Calculation Results of the Contribution Coefficients μ_2 weighting coefficients $\gamma_{t,2}$ and $\gamma_{x,2}$.

ε	μ_2	$\gamma_{t,2}$	$\gamma_{x,2}$
0.01	-0.001067	1.998933	0.998933
0.02	-0.004267	1.995733	0.995733
0.03	-0.009600	1.990400	0.990400
0.04	-0.017067	1.982933	0.982933
0.05	-0.026667	1.973333	0.973333
0.06	-0.038400	1.961600	0.961600
0.07	-0.052267	1.947733	0.947733
0.08	-0.068267	1.931733	0.931733
0.09	-0.086400	1.913600	0.913600
0.1	-0.106667	1.893333	0.893333

Table (2) shows that as the optimization coefficient ε increases, the value of $|\mu_2|$ also increases. This indicates that the contribution of the third-order odd differential term becomes more significant.

III. THE FORMULATION OF WEIGHTED TAYLOR SERIES 3-D

Taylor series for functions with 3 variable $f = f(x, z, t)$ is, $f(x + \delta x, z + \delta z, t + \delta t) = f(x, z, t) + s_1 + s_2 + s_3 \dots \dots + s_n$

Where,

$$s_1 = \delta t \frac{\partial f}{\partial t} + \delta x \frac{\partial f}{\partial x} + \delta z \frac{\partial f}{\partial z}$$

$$s_2 = \frac{\delta t^2}{2!} \frac{\partial^2 f}{\partial t^2} + \delta t \delta x \frac{\partial^2 f}{\partial t \partial x} + \delta t \delta z \frac{\partial^2 f}{\partial t \partial z} + \frac{\delta x^2}{2!} \frac{\partial^2 f}{\partial x^2} + \delta x \delta z \frac{\partial^2 f}{\partial x \partial z} + \frac{\delta z^2}{2!} \frac{\partial^2 f}{\partial z^2}$$

Etc.

Odd differential terms are grouped

$$f(x + \delta x, z + \delta z, t + \delta t) = f(x, z, t) + s_1 + s_2 + s_4 + s_6 \dots + \sum_{j=2i+1}^{2n+1} s_j$$

Where i ranges from 1 to n .

For,

$$\sum_{j=2i+1}^{2n+1} s_j = \mu_3 s_1 \quad \dots \dots (16)$$

Taylor series can be reformulated into,

$$f(x + \delta x, z + \delta z, t + \delta t) = f(x, z, t) + (1 + \mu_3) s_1 + s_2 + s_4 + s_6 \dots \dots (17)$$

Expansion is then performed to $(x - \delta x, z - \delta z, t - \delta t)$, yielding

$$f(x - \delta x, z - \delta z, t - \delta t) = f(x, z, t) - (1 + \mu_3) s_1$$

$$+s_2 + s_4 + s_6 + \dots \quad (18)$$

Equation (17) is subtracted by equation (18),

$$f(x + \delta x, z + \delta z, t + \delta t) - f(x - \delta x, z - \delta z, t - \delta t) = 2(1 + \mu_3)s_1$$

s_1 is broken down,

$$f(x + \delta x, z + \delta z, t + \delta t) - f(x - \delta x, z - \delta z, t - \delta t) = 2(1 + \mu_3)\delta t \frac{\partial f}{\partial t} + 2(1 + \mu_3)\delta x \frac{\partial f}{\partial x} + 2(1 + \mu_3)\delta z \frac{\partial f}{\partial z} \quad (19)$$

This equation represents the total change in the function value as it transitions from $(t - \delta t, x - \delta x, z - \delta z)$ to $(t + \delta t, x + \delta x, z + \delta z)$

Equation (19) is divided by $2 \delta x$,

$$\frac{f(t + \delta t, x + \delta x, z + \delta z) - f(t - \delta t, x - \delta x, z - \delta z)}{2\delta x} = (1 + \mu_3) \frac{\delta t}{\delta x} \frac{\partial f}{\partial t} + (1 + \mu_3) \frac{\partial f}{\partial x} + (1 + \mu_3) \frac{\delta z}{\delta x} \frac{\partial f}{\partial z}$$

This equation represents the change in the function value in the $-x$ axis direction per unit length. As δt , δx and δz approach zero, the total differential in the $-x$ axis is:

$$\frac{Df}{dx} = (1 + \mu_3) \frac{\delta t}{\delta x} \frac{\partial f}{\partial t} + (1 + \mu_3) \frac{\partial f}{\partial x} + (1 + \mu_3) \frac{\delta z}{\delta x} \frac{\partial f}{\partial z} \quad \dots (20)$$

Similarly, the total differential in the $-z$ axis is,

$$\frac{Df}{dz} = (1 + \mu_3) \frac{\delta t}{\delta z} \frac{\partial f}{\partial t} + (1 + \mu_3) \frac{\delta x}{\delta z} \frac{\partial f}{\partial x} + (1 + \mu_3) \frac{\partial f}{\partial z} \quad \dots (21)$$

The first-order Taylor series expansion is:

$$f(t + \delta t, x + \delta x, z + \delta z) = f(t, x, z) + \delta t \frac{\partial f}{\partial t} + \delta x \frac{\partial f}{\partial x} + \delta z \frac{\partial f}{\partial z}$$

$\frac{\partial f}{\partial x}$ in the 3rd term is substituted by (20) and $\frac{\partial f}{\partial z}$ the third term of the right side is substituted by (21),

$$f(t + \delta t, x + \delta x, z + \delta z) = f(t, x, z) + (3 + 2\mu_3)\delta t \frac{\partial f}{\partial t} + (2 + 2\mu_3)\delta x \frac{\partial f}{\partial x} + (2 + 2\mu_3)\delta z \frac{\partial f}{\partial z}$$

Defined as,

$$\gamma_{t,3} = 3 + 2\mu_3$$

$$\gamma_{x,3} = 2 + 2\mu_3$$

$$\gamma_{z,3} = 2 + 2\mu_3$$

Therefore,

$$f(t + \delta t, x + \delta x, z + \delta z) = f(t, x, z) + \gamma_{t,3}\delta t \frac{\partial f}{\partial t} + \gamma_{x,3}\delta x \frac{\partial f}{\partial x} + \gamma_{z,3}\delta z \frac{\partial f}{\partial z} \quad \dots (22)$$

This equation represents a weighted Taylor series expansion for the function $f = f(x, z, t)$, with weighting coefficients $\gamma_{t,3}$, $\gamma_{x,3}$ and $\gamma_{z,3}$.

The calculation of the grid coefficients ϵ_t and ϵ_x follows the same method as the calculation for the function $f = f(x, t)$, while the equation for ϵ_z is formulated similarly to that of ϵ_x , by using the optimization equation:

$$\left| \frac{s_2}{s_1} \right| < \epsilon$$

Substituting s_1 and s_2 ,

$$s_1 = \delta t \frac{\partial f}{\partial t} + \delta x \frac{\partial f}{\partial x} + \delta z \frac{\partial f}{\partial z}$$

$$s_2 = \frac{\delta t^2}{2!} \frac{\partial^2 f}{\partial t^2} + \delta t \delta x \frac{\partial^2 f}{\partial t \partial x} + \delta t \delta z \frac{\partial^2 f}{\partial t \partial z} + \frac{\delta x^2}{2!} \frac{\partial^2 f}{\partial x^2} + \delta x \delta z \frac{\partial^2 f}{\partial x \partial z} + \frac{\delta z^2}{2!} \frac{\partial^2 f}{\partial z^2}$$

Substituting

$f(x, z, t) = \cos \sigma t \cos kx \cosh k(h + z)$ under $\cos \sigma t = \sin \sigma t$, $\cos kx = \sin kx$ and $\cosh k(h + z) = \sinh k(h + z)$. Substituting $\delta t = \epsilon_t T$, $\delta x = \epsilon_x L$ and $\delta z = \epsilon_z L$ serta $\sigma = \frac{2\pi}{T}$ and $k = \frac{2\pi}{L}$ yields the equation:

$$\frac{1}{2} \epsilon_z^2 - \left(\epsilon_t + \epsilon_x + \frac{\epsilon}{2\pi} \right) \epsilon_z - \frac{\epsilon_t^2}{2} + \epsilon_t \epsilon_x - \frac{\epsilon_x^2}{2} + \frac{\epsilon \epsilon_t}{2\pi} + \frac{\epsilon \epsilon_x}{2\pi} = 0 \quad \dots (23)$$

In this equation, ϵ_t and ϵ_x are known constants, with ϵ_t is calculated using equation (14) and ϵ_x is calculated by (15). The equation has two roots, and the largest root is chosen.

The equation for calculating the contribution coefficient μ_3 is formulated in the same manner as for μ_2 . Yielding,

$$\mu_3 = \frac{a}{b} \quad \dots (24)$$

$$a = \frac{(2\pi)^3}{6} \epsilon_t^3 + \frac{(2\pi)^3}{2} \epsilon_t^2 \epsilon_x - \frac{(2\pi)^3}{2} \epsilon_t^2 \epsilon_z + \frac{(2\pi)^3}{2} \epsilon_t \epsilon_x^2 + (2\pi)^3 \epsilon_t \epsilon_x \epsilon_z - \frac{(2\pi)^3}{2} \epsilon_t \epsilon_z^2 + \frac{(2\pi)^3}{6} \epsilon_x^3 - \frac{(2\pi)^3}{2} \epsilon_x^2 \epsilon_z - \frac{(2\pi)^3}{2} \epsilon_x \epsilon_z^2 + \frac{(2\pi)^3}{6} \epsilon_z^3$$

$$b = -2\pi \epsilon_t - 2\pi \epsilon_x + 2\pi \epsilon_z$$

Table (3) Values of ε_z and μ_3

ε	ε_z	μ_3
0.01	0.028648	0.049333
0.02	0.057296	0.098667
0.03	0.085944	0.148000
0.04	0.114592	0.197333
0.05	0.143239	0.246667
0.06	0.171887	0.296000
0.07	0.200535	0.345333
0.08	0.229183	0.394667
0.09	0.257831	0.444000
0.1	0.286479	0.493333

Table (4) Values of $\gamma_{t,3}$, $\gamma_{x,3}$ and $\gamma_{z,3}$

ε	$\gamma_{t,3}$	$\gamma_{x,3}$	$\gamma_{z,3}$
0.01	3.098667	2.098667	2.098667
0.02	3.197333	2.197333	2.197333
0.03	3.296000	2.296000	2.296000
0.04	3.394667	2.394667	2.394667
0.05	3.493333	2.493333	2.493333
0.06	3.592000	2.592000	2.592000
0.07	3.690667	2.690667	2.690667
0.08	3.789333	2.789333	2.789333
0.09	3.888000	2.888000	2.888000
0.1	3.986667	2.986667	2.986667

IV. WAVE CONSTANT EQUATIONS IN DEEP WATER

The continuity equation, as formulated in Equation (22), where $\gamma_{x,3} = \gamma_z$ no longer represents a weighted continuity equation, nor does it take the form of a weighted Laplace equation as discussed in Hutahaean (2023a). The velocity potential derived from solving the Laplace equation via the method of variable separation (Dean, 1991) is given by:

$$\phi(x, z, t) = G(\cos kx + \sin kx) \cosh k(h + z) \sin \sigma t \dots (25)$$

Where,

x is the horizontal coordinate, z is the vertical axis and t is time.

G : is the wave constant

k : is the wave number, $k = \frac{2\pi}{L}$, L is wavelength

σ : is angular frequency, $\sigma = \frac{2\pi}{T}$, T is wave period.

There are three wave constants: G, k and σ , equation of which must be determined.

a. Wave Amplitude Function

At the characteristic point where $\cos kx = \sin kx$, the velocity potential equation becomes:

$$\phi(x, z, t) = 2G \cos kx \cosh k(h + z) \sin \sigma t \dots (26)$$

By applying the Kinematic Free Surface Boundary Condition (Equation 10), the following is obtained

$$w_\eta = \gamma_{t,2} \frac{\partial \eta}{\partial t} + \gamma_{x,2} u_\eta \frac{\partial \eta}{\partial x}$$

This equation can be reformulated into,

$$\gamma_{t,2} \frac{\partial \eta}{\partial t} = w_\eta - \gamma_{x,2} u_\eta \frac{\partial \eta}{\partial x} \dots (27)$$

$\eta(x, t)$ is the water surface elevation relative to the still water level, $w_\eta(x, t)$ is the vertical velocity of surface water particles, $u_\eta(x, t)$ is the horizontal velocity of surface water particles.

Substituting (26) into (27) where $u = -\frac{\partial \phi}{\partial x}$ and $w = -\frac{\partial \phi}{\partial z}$ and integrating to t obtaining a wave amplitude function Hutahaean (2023b),

$$A = \frac{2Gk}{\gamma_{t,2}\sigma} \cosh \theta\pi \left(\tanh \theta\pi - \frac{\gamma_{x,2}kA}{2} \right) \dots (28)$$

A is wave amplitude, θ is deep water coefficient, where $\tanh \theta\pi \approx 1$. In this research, $\theta = 3$ is used to keep the deep water sea bed horizontal particle velocity very small and to avoid large wave amplitude in the coastline.

A new wave constant amplitude A is obtained. In this research, wave amplitude A is the input, therefore wave amplitude A is an identified variable.

The next step involves formulating the wave constant equations for σ, k and G as the function of wave amplitude A .

b. Formulation of equation for G .

In this section, the complete velocity potential equation is applied to the Kinematic Free Surface Boundary Condition to derive wave constant equations consistent with the complete velocity potential. The formulation re-employs the Kinematic Free Surface Boundary Condition to ensure that the derived wave constant equations are rigorously aligned with this boundary condition. Through the utilization of the complete velocity potential, the corresponding water surface elevation equation is formulated as follows:

$$\eta(x, t) = \frac{Gk}{\gamma_{t,2}\sigma} \sinh k(h + \eta) (\cos kx + \sin kx) \cos \sigma t$$

$$+ \frac{\gamma_x G k}{\gamma_{t,2}\sigma} \cosh k(h + \eta) \frac{\partial \eta}{\partial x} (-\sin kx + \cos kx) \cos \sigma t$$

η maximum when $\frac{d\eta}{dx} = 0$ and $\cos \sigma t = 1$, where for sinusoidal wave $\eta_{max} = A$, the following relation is obtained

$$A = \frac{Gk}{\gamma_{t,2}\sigma} \sinh k(h + \eta) (\cos kx + \sin kx)$$

At $\cos kx = \sin kx$ and $k(h + \eta) = \theta\pi$, therefore

$$A = \frac{\sqrt{2} Gk}{\gamma_{t,2}\sigma} \sinh \theta\pi \dots (29)$$

This equation can be reformulated into equation for G as follows.

$$G = \frac{\gamma_{t,2}\sigma A}{\sqrt{2} k \sinh \theta\pi} \dots (30)$$

c. Formulation of the Deep Water Wave Number k equation

By equating Equation (28) with Equation (29), the equation for the wave number k is

$$k = \frac{\tanh \theta\pi}{\gamma_{x,2}A} (2 - \sqrt{2}) \dots (31)$$

d. Formulation of the Equation for Wave Period T .

The Euler momentum conservation equation is employed, with the assumption that convective acceleration is negligible,

$$\gamma_{t,3} \frac{\partial u_\eta}{\partial t} = -g \frac{\partial \eta}{\partial x} \dots (32)$$

u is horizontal particle velocity where $u = -\frac{\partial \phi}{\partial x}$, is potential velocity ϕ using (26).

For water surface elevation equation, the following is used:
 $\eta(x, t) = A \cos kx \cos \sigma t$

Obtaining an equation,

$$\gamma_{t,3} 2G\sigma \cosh \theta\pi = gA$$

Substituting A to (29) yielding:

$$\sigma^2 = \frac{gk \tanh \theta\pi}{\sqrt{2}\gamma_{t,2}\gamma_{t,3}} \dots (33)$$

Substituting k and (31),

$$\sigma^2 = \frac{g \tanh^2 \theta\pi}{\gamma_{t,2}\gamma_{t,3}\gamma_{x,2}A} (\sqrt{2} - 1) \dots (34)$$

e. Results of Deep Water Wave Constants Equations.

In this section, the calculation results of deep water wave constants, including the wave period T and wavelength L_0 using input wave amplitude A_0 where $H_0 = 2A_0$. Table (5) presents the result.

The weighting coefficients used in these calculations are obtained through the optimization process, with an optimization coefficient $\varepsilon = 0.005$, where $\gamma_{t,2} = 1.999773$, $\gamma_{t,3} = 3.049333$, $\gamma_x = 0.999733$. These coefficients will be applied in subsequent equations in this research.

Table (5) Deep water wave constants

H_0 (m)	T (sec)	L_0 (m)	$\frac{H_0}{L_0}$
0.4	3.442	2.145	0.187
0.8	4.867	4.289	0.187
1.2	5.961	6.434	0.187
1.6	6.883	8.579	0.187
2	7.696	10.723	0.187
2.4	8.431	12.868	0.187
2.8	9.106	15.012	0.187
3.2	9.735	17.157	0.187
3.6	10.325	19.302	0.187
4	10.884	21.446	0.187

The wave steepness, $\frac{H_0}{L_0}$, where $\frac{H_0}{L_0} = 0.187$. When compared with the critical wave steepness criterion from Toffoli et al. (2010), where $\frac{H_0}{L_0} = 0.170$ it is evident that the calculated wave steepness is slightly larger. This indicates that the wavelength equation (31) produces a critical wave steepness for a given input wave amplitude.

To further assess the condition of the resulting wave period, a comparison is made with the wave period equation from Wiegel (1949, 1964), given by:

$$T_{wieg} = 15.6 \sqrt{\frac{H_0}{g}} \dots (35)$$

The comparison is presented in Table(6) and Fig (1)

Table (6) The Comparison to Wiegel's Wave Period.

H_0 (m)	T (sec)	T_{wieg} (sec)	δ (%)
0.4	3.442	3.15	9.259
0.8	4.867	4.455	9.259
1.2	5.961	5.456	9.259
1.6	6.883	6.3	9.259
2	7.696	7.044	9.259
2.4	8.431	7.716	9.259

2.8	9.106	8.334	9.259
3.2	9.735	8.91	9.259
3.6	10.325	9.45	9.259
4	10.884	9.961	9.259

Note : $\delta = \left| \frac{T_0 - T_{0-wieg}}{T_0 - Wieg} \right| \times 100\%$

T from equation (34) differs by 9.259% from the wave period in Wiegel’s formulation, a difference considered reasonable, indicating that the result from equation (34) is still reliable. If the right side of equation (34) is multiplied by 1.2116, the wave period would match that of equation (35). However, the goal of this research is not to match the wave period in equation (35), but to explore the potential within the existing conservation equations. Equation (35) does not guarantee exact correct wave period.

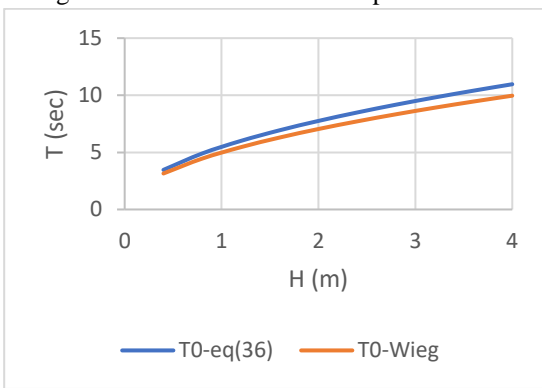


Fig (1) Comparison of wave period eq (34) with Wiegel’s wave period.

Equation (34) shows that all the weighting coefficients are included, making the equation sensitive to their values. As the optimization coefficient ϵ decreases, the difference from the Wiegel equation also decreases, but it remains around 8.xxx%. For example, $\epsilon = 0.001$ results in a difference of $\delta = 8.571\%$, with a wave steepness of 0.187. Therefore, this research uses the weighting coefficients obtained with $\epsilon = 0.005$, ensuring that the influence of higher-order differentials on the coefficients is not entirely lost.

V. SHOALING-BREAKING MODEL

The shoaling-breaking model is formulated using the wave amplitude function (eq. (28)) as follows.

$$A = \frac{2Gk}{\gamma_{t,2}\sigma} \cosh \theta\pi \left(\tanh \theta\pi - \frac{\gamma_{x,2}kA}{2} \right) \dots (28)$$

To make formulation easier, it is defined

$$\lambda = \frac{1}{\gamma_{t,2}\sigma} \cosh \theta\pi \left(\tanh \theta\pi - \frac{\gamma_{x,2}kA}{2} \right) \dots (36)$$

Thereby,

$$A = 2Gk\lambda \dots (37)$$

Differentiation of the Wave Amplitude with respect to the Horizontal -x,

$$\frac{dA}{dx} = 2 \left(G \frac{dk}{dx} + k \frac{dk}{dx} \right) \lambda \dots (38)$$

Where $\frac{d\lambda}{dx} = 0$ with respect to wave number conservation equation (Hutahaean (2023b)), $\frac{dkA}{dx} = 0$.

Equation of energy conservation (Hutahaean (2023b)),

$$G \frac{\partial k}{\partial x} + 2k \frac{\partial G}{\partial x} = 0 \dots (39)$$

Or

$$\frac{\partial G}{\partial x} = - \frac{G}{2k} \frac{\partial k}{\partial x}$$

Substituting the last equation to (38),

$$\frac{dA}{dx} = G \frac{dk}{dx} \lambda \dots (40)$$

The equation of wave number conservation (Hutahaean, 2023b) is expressed as

$$\frac{dk \left(h + \frac{A}{2} \right)}{dx} = 0$$

This equation can be reformulated into,

$$k \frac{dA}{dx} = -2 \left(h + \frac{A}{2} \right) \frac{dk}{dx} - 2k \frac{dh}{dx}$$

Substituting the left-hand side with Equation (40), this leads to the following equation for $\frac{dk}{dx}$,

$$\frac{dk}{dx} = - \frac{k}{h + \frac{A}{2} + \frac{Gk\lambda}{2}} \frac{dh}{dx} \dots (41)$$

a. Summary of Shoaling-Breaking Equations.

For waves moving from a point x and water depth h_x to $x + \delta x$ and water depth $h_{x+\delta x}$, therefore

a. Change in Wave Number:

$$\frac{dk}{dx} = - \frac{k}{h + \frac{A}{2} + \frac{Gk\lambda}{2}} \frac{dh}{dx} \dots (41)$$

$$k_{x+\delta x} = k_x + \delta x \frac{dk}{dx}$$

b. Change in wave amplitude

$$\frac{dA}{dx} = \frac{G}{2k} \frac{\partial k}{\partial x} \lambda \dots (40)$$

$$\lambda = \frac{1}{\gamma_{t,2}\sigma} \cosh \theta\pi \left(\tanh \theta\pi - \frac{\gamma_{x,2}kA}{2} \right) \dots (36)$$

$$A_{x+\delta x} = A_x + \delta x \frac{dA}{dx}$$

c. Change in wave constant G

Integration of energy conservation equation (39),

$$G_{x+\delta x} = e^{\ln G_x - \frac{1}{2}(\ln k_{x+\delta x} - \ln k_x)}$$

d. Change in wave energy

The wave energy equation at one wavelength is given by

$$E = \frac{1}{8} \rho g H^2 L$$

Or,

$$E = \pi \rho g \frac{A^2}{k}$$

The wave energy change is,

$$\frac{dE}{dx} = \pi \rho g \left(\frac{2A}{k} \frac{dA}{dx} - \frac{A^2}{k^2} \frac{dk}{dx} \right) \quad \dots (42)$$

$$E_{x+\delta x} = E_x + \delta x \frac{dE}{dx}$$

Where $\frac{dA}{dx}$ from (40) and $\frac{dk}{dx}$ dari (41).

b. Shoaling-Breaking Model Results.

The results of the shoaling-breaking model for a wave with a deep water amplitude $A_0 = 1.20 \text{ m}$ are shown in the following section. The deep water coefficient is set at $\theta = 3$, and the optimization coefficient used for calculating the weighting coefficients is $\varepsilon = 0.005$.

In Fig (2), the wave height H and $0.1 H^2 L$, are plotted against water depth. The factor of $0.1 H^2 L$ is used to prevent the H from having smaller value.

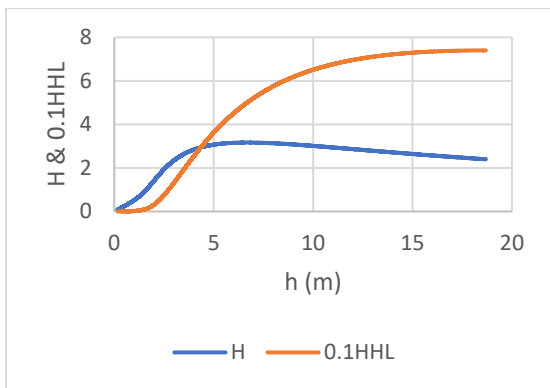


Fig (2) Changes in wave energy during shoaling and breaking

Fig (2) illustrates that the value of $H^2 L$ decreases continuously as the wave enters shallow water, which corresponds to the shoaling process. At a water depth of $h = 6.669 \text{ m}$ wave breaking occurs. Notably, the $H^2 L$ graph remains continuous at the breaking point, and no sudden spike in energy loss is observed. The remaining wave

energy at this point is calculated to be $0.675 E_0$ as shown in Table (7).

Table (7) Wave Energy at the Breaking Point

T (sec)	H_0 (m)	H_b (m)	h_b (m)	$\frac{E_b}{E_0}$
0.4	3.467	0.528	1.111	0.675
0.8	4.904	1.057	2.223	0.675
1.2	6.006	1.585	3.334	0.675
1.6	6.935	2.113	4.446	0.675
2	7.753	2.642	5.557	0.675
2.4	8.493	3.17	6.669	0.675
2.8	9.174	3.698	7.78	0.675
3.2	9.807	4.227	8.892	0.675
3.6	10.402	4.755	10.003	0.675
4	10.965	5.283	11.115	0.675

c. Shoaling-Breaking Model Evaluation

To assess the reliability of the shoaling-breaking model developed in this research, a comparison was made between the breaking wave height calculated using the model and the breaking wave height obtained from the Komar and Gaughan (1972) equation. The equation used for comparison is:

$$H_{b-KG} = 0.39 g^{1/5} (T_0 H_0^2)^{2/5} \quad \dots (43)$$

Table (8): Evaluation of the Shoaling-Breaking Model Breaker Height Against the Komar-Gaughan Breaker Height

H_0 (m)	T (sec)	H_b (m)	H_{b-KG} (m)	δ (%)
0.4	3.467	0.528	0.486	8.606
0.8	4.904	1.057	0.973	8.606
1.2	6.006	1.585	1.459	8.606
1.6	6.935	2.113	1.946	8.606
2	7.753	2.642	2.432	8.606
2.4	8.493	3.17	2.919	8.606
2.8	9.174	3.698	3.405	8.606
3.2	9.807	4.227	3.892	8.606
3.6	10.402	4.755	4.378	8.606
4	10.965	5.283	4.865	8.606

Note : $\delta = \left| \frac{H_b - H_{b-KG}}{H_{b-KG}} \right| \times 100\%$

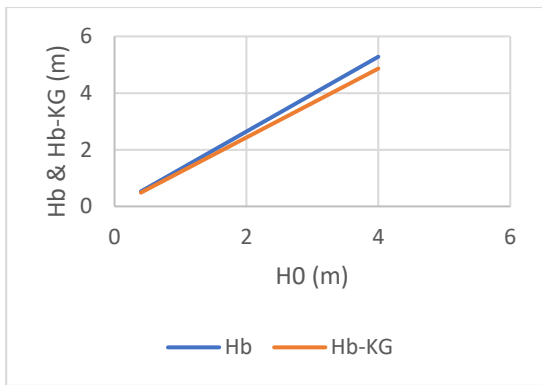


Fig (3) The comparison of the breaker heights predicted by the shoaling-breaking model and the Komar-Gaughan method.

The observed difference is 8.608 (moderate).

d. Energy Loss Evaluation.

In the context of energy loss during shoaling and breaking, the remaining wave energy at the breaking point is found to be $0.675 E_0$, where E_0 represents the initial wave energy in deep water. To further evaluate the accuracy of energy loss, the breaking wave height equation is formulated using the energy loss equation:

$$H_b^2 L_b = 0.675 H_0^2 L_0 \quad \dots (44)$$

From equation (31), breaking occurs when

$$\tanh \theta \pi - \frac{\gamma_{x,2} k A}{2} = 0$$

This equation yields,

$$L_b = \frac{\pi \gamma_{x,2} H_b}{2 \tanh \theta \pi} \quad \dots (45)$$

Substituting (45) to (44),

$$H_b^3 = \frac{2 \times 0.675 \tanh \theta \pi}{\pi \gamma_{x,2}} H_0^2 L_0 \quad \dots (46)$$

From (31),

$$L_0 = \frac{\pi \gamma_{x,2} H_0}{(2 - \sqrt{2}) \tanh \theta \pi} \quad \dots (47)$$

Substituting (47) to (46) obtains,

$$H_b = \left(\frac{0.675}{\left(1 - \frac{1}{\sqrt{2}}\right)} \right)^{1/3} H_0 \quad \dots (48)$$

Table (9) The Comparison between H_{b-48} , eq(48), and H_b -Komar-Gaughan

H_0 (m)	T (sec)	H_{b-48} (m)	H_{b-KG} (m)	δ (%)
0.4	3.467	0.528	0.486	8.612

0.8	4.904	1.057	0.973	8.612
1.2	6.006	1.585	1.459	8.612
1.6	6.935	2.113	1.946	8.612
2	7.753	2.642	2.432	8.612
2.4	8.493	3.17	2.919	8.612
2.8	9.174	3.698	3.405	8.612
3.2	9.807	4.227	3.892	8.612
3.6	10.402	4.755	4.378	8.612
4	10.965	5.284	4.865	8.612

Note : $\delta = \left| \frac{H_{b-50} - H_{b-KG}}{H_{b-KG}} \right| \times 100\%$

Upon comparing the breaking wave heights calculated from the energy loss equation H_{b-48} that is H_b -eq(48) and H_b -Komar-Gaughan (Table (9)), it is observed that both produce breaker heights that are close. This indicates that the shoaling-breaking model, which uses wave energy loss as part of its formulation, yields accurate results for the breaking wave height. Since H_{b-48} is derived using the energy loss during shoaling and breaking, the close agreement between the two sets of results suggests that the model effectively accounts for wave energy loss.

The loss of energy during shoaling and breaking processes is converted into kinetic energy for non-orbital currents, known as stress radiation (Longuet-Higgin, 1970), with some of this energy transforming into longshore currents. The shoaling-breaking model accurately estimates the kinetic energy of these longshore currents, and its ability to predict their velocity is crucial for understanding coastal dynamics, such as sediment transport and shoreline changes.

VI. LONGSHORE CURRENT ANALYSIS

Wave energy lost during shoaling and breaking is converted into the kinetic energy of non-orbital currents that move in the same direction as the wave. This release of wave energy is known as stress radiation.

The loss of wave energy at one wavelength is expressed by (42), then the water particle energy losses is

$$\delta E_w = \frac{dE}{dx} \rho L$$

The energy kinetic particle due to radiation current,

$$E_k = \frac{V_k^2}{2g}$$

Then this equation applies,

$$\frac{V_R^2}{2g} = \left| \frac{dE}{dx} \right| \left| \frac{1}{\rho L} \right|$$

Substituting (42)

$$V_R^2 = \frac{2\pi g^2}{L} \left| \frac{2A dA}{k dx} - \frac{A^2 dk}{k^2 dx} \right| \quad \dots (49)$$

V_R is the total velocity of the radiation current. For waves that form an angle α to the normal of the coast, the longshore current velocity is:

$$V_{Ls} = V_R \sin \alpha \quad \dots (50)$$

An example of the radiation current velocity analysis V_R is shown in Figure (4), where the waves used have a deep-water wave height $H_0 = 2.4 \text{ m}$, with breaking occurring at a breaker depth of $h_b = 6.669 \text{ m}$.

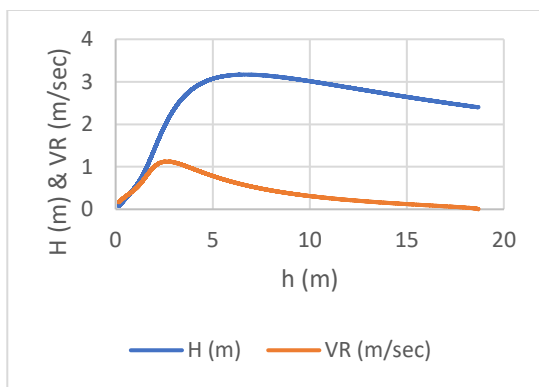


Fig (4) Stress radiation current velocity V_R .

Similar to the wave energy graph, this radiation current graph is continuous, with no spike at the breaking point. The highest velocity is 1.13 m/sec, occurring at a water depth of $h = 2.65 \text{ m}$, while at the breaker depth of $h_b = 6.669 \text{ m}$, velocity $V_R = 0.57 \text{ m/sec}$. Notably, the maximum velocity does not occur at the breaking point. As shown in Figure (4), the maximum velocity occurs at a depth where the wave height has decreased significantly.

Table (10) presents the radiation current velocities at different wave periods. It shows that the maximum current velocity does not occur at the breaking point, but rather at a shallower water depth than the breaker depth. For example, with a deep-water wave height $H_0 = 2.0 \text{ m}$, V_R the radiation current velocity at the breaking point $V_{R-b} = 0.52 \text{ m/sec}$ at a breaker depth of $h_b = 5.56 \text{ m}$, while the maximum velocity $V_{max} = 1.03 \text{ m/sec}$, occurs at a shallower water depth of $h_{vmx} = 2.21 \text{ m}$.

Table (10): Velocity V_R at breaking point V_{R-b} and maximum speed V_{max} .

H_0 (m)	T (sec)	V_{R-b} (m)	h_b (m/s)	V_{max} (m/s)	h_{vmx} (m)
0.4	3.47	0.23	1.11	0.46	0.44
0.8	4.9	0.33	2.22	0.65	0.88
1.2	6.01	0.4	3.33	0.8	1.33
1.6	6.93	0.46	4.45	0.92	1.77
2	7.75	0.52	5.56	1.03	2.21
2.4	8.49	0.57	6.67	1.13	2.65
2.8	9.17	0.61	7.78	1.22	3.09
3.2	9.81	0.66	8.89	1.3	3.53
3.6	10.4	0.7	10	1.38	3.98
4	10.96	0.73	11.11	1.45	4.42

a. Results of Prior Research

The theory of stress radiation was first proposed by Longuet-Higgin (1970), which describes how wave energy, transferred through the orbital motion of water particles, is converted into non-orbital currents moving in the same direction as the wave. Based on this theory, the longshore current equation was formulated. Several researchers have developed longshore current equations based on Longuet-Higgins' theory, which are widely used in the field:

1. Komar (1976), modified Longuet Higgins

$$V_{Kom} = 2.7 \left(\frac{\gamma_b}{2} \sqrt{gH_b} \right) \sin \alpha_b \cos \alpha_b$$

Where $\gamma_b = 0.78$

2. Galvin, C. (1987)

$$V_{Gal} = g m T \sin 2\alpha_b$$

T : wave period

m : bottom slope

Table (11) presents a comparison of the longshore current velocity model results at the breaking point V_{L-b} as derived from the model and the equations from Komar and Galvin, using an angle $\alpha_b = 15^\circ$, resulting in model V_{L-b} as the smallest among the three methods..

Table (11) Comparison longshore current velocity at breaking point.

T (sec)	H_b (m)	V_{Kom} (m/sec)	V_{Gal} (m/sec)	V_{L-b} (m/sec)
3.47	0.53	0.6	0.17	0.06
4.9	1.06	0.85	0.24	0.09

6.01	1.58	1.04	0.29	0.1
6.93	2.11	1.2	0.34	0.12
7.75	2.64	1.34	0.38	0.13
8.49	3.17	1.47	0.42	0.15
9.17	3.7	1.59	0.45	0.16
9.81	4.23	1.7	0.48	0.17
10.4	4.75	1.8	0.51	0.18
10.96	5.28	1.9	0.54	0.19

Table (12) compares the longshore current velocities from Komar and Galvin with the maximum velocity from the model. As seen in the table, the model results are still the smallest, but they are quite close to the longshore current velocity from Galvin.

Table (12) Comparison with the maximum velocity.

T (sec)	H_b (m)	V_{Kom} (m/sec)	V_{Gal} (m/sec)	V_{L-max} (m/sec)
3.47	0.53	0.6	0.17	0.12
4.9	1.06	0.85	0.24	0.17
6.01	1.58	1.04	0.29	0.21
6.93	2.11	1.2	0.34	0.24
7.75	2.64	1.34	0.38	0.27
8.49	3.17	1.47	0.42	0.29
9.17	3.7	1.59	0.45	0.31
9.81	4.23	1.7	0.48	0.34
10.4	4.75	1.8	0.51	0.36
10.96	5.28	1.9	0.54	0.38

However, velocities from the model and Galvin's equation occur at different water depths.

There is a significant difference between the model results and those from previous equations. The previous equations are applied to the breaker depth, whereas the maximum velocity in the model occurs at a shallower depth, not at the breaker depth.

Nevertheless, the analysis of breaker height and the remaining wave energy at the breaking point validates the accuracy of the wave energy release in the shoaling and breaking model, which in turn confirms the accuracy of the resulting longshore current.

The calculations in Table (12) are performed using a deep-water coefficient of $\theta = 3.0$. In Table (13), with a coefficient $\theta = 1.95$, where $\frac{H_b}{h_b} \approx 0.78$, V_{L-max} is found

close to V_{Gal} , however these velocities occur at different water depths. V_{Gal} occurs at the breaker depth, while V_{L-max} occurs at a shallower water depth (see Table (10)).

Table (13) Comparison longshore current velocity at $\theta = 1.95$.

T (sec)	H_b (m)	V_{Kom} (m/sec)	V_{Gal} (m/sec)	V_{L-max} (m/sec)
3.47	0.53	0.6	0.17	0.16
4.9	1.06	0.85	0.24	0.22
6.01	1.58	1.04	0.29	0.27
6.93	2.11	1.2	0.34	0.31
7.75	2.64	1.34	0.38	0.35
8.49	3.17	1.47	0.42	0.39
9.17	3.7	1.59	0.45	0.42
9.81	4.23	1.7	0.48	0.44
10.4	4.75	1.8	0.51	0.47
10.96	5.28	1.9	0.54	0.5

VII. CONCLUSION

This research shows that the method used to formulate the weighting coefficient in the weighted Taylor series is more systematic and accurate compared to the previous approach by the same researcher. By applying the correct weighting coefficient, the resulting weighted Taylor series effectively represents the complete Taylor series.

The development of the shoaling-breaking model through the application of the weighted Taylor series yields accurate predictions for both the breaker height and the remaining energy at the breaking point. Therefore, it can be concluded that the shoaling-breaking model in this research successfully simulates the release of wave energy, or stress radiation, with high fidelity. Moreover, given the appropriate kinetic energy supply from the shoaling-breaking model, it can be concluded that the longshore current produced by the model is accurate.

The maximum longshore current velocity does not occur at the breaking point. Instead, it is observed at a shallower depth than the breaker depth, specifically at a depth where a significant reduction in wave energy occurs.

REFERENCES

[1] Longuet Higgins, MS (1970). Longshore current generated by Obliquely Incident wave, 1. J.Geophysics. Res., 75, 6778-6789.
 [2] Arden, Bruce W. and Astill Kenneth N. (1970). Numerical Algorithms : Origins and Applications. Philippines copyright (1970) by Addison-Wesley Publishing Company, Inc.

- [3] Courrant, R., Friedrichs, K., Lewy, H. (1928). Uber die Partiellen Differenzengleichungen der mathematischen Physik. *Mathematischen Annalen* (in German). 100 (1);32-74, Bibcode : 1928,MatAn. 100.32.c. doi: 10.1007/BF01448839, JFM 54.0486.01 MR 1512478.
- [4] Hutahaean, S. (2023a). Method for Determining Weighting Coefficients in Weighted Taylor Series Applied to Water Wave Modeling. *International Journal of Advance Engineering Research and Science (IJAERS)*. Vol. 10, Issue 12; Dec, 2023, pp 105-114. Article DOI: <https://dx.doi.org/10.22161/ijaers.1012.11>.
- [5] Dean, R.G., Dalrymple, R.A. (1991). *Water wave mechanics for engineers and scientists*. Advance Series on Ocean Engineering.2. Singapore: World Scientific. ISBN 978-981-02-0420-4. OCLC 22907242.
- [6] Hutahaean, S. (2023b). Water Wave Velocity Potential on Sloping Bottom in Water Wave Transformation Modeling . *International Journal of Advance Engineering Research and Science (IJAERS)*. Vol. 10, Issue 10; Oct, 2023, pp 149-157. Article DOI: <https://dx.doi.org/10.22161/ijaers.1010.15>.
- [7] Toffoli, A., Babanin, A., Onaroto, M. and Wased, T. (2010). Maximum steepness of oceanic waves : Field and laboratory experiments. *Geophysical Research Letters*. First published 09 March 2010. <https://doi.org/10.1029/2009GL.0441771>
- [8] Wiegel, R.L. (1949). An Analysis of Data from Wave Recorders on the Pacific Coast of the United States, *Trans. Am. Geophys. Union*, Vol.30, pp.700-704.
- [9] Komar, P.D. & Gaughan M.K. (1972). Airy Wave Theory and Breaker Height Prediction, *Coastal Engineering Proceedings*, 1 (13).
- [10] Komar, P.D (1976). *Beach processes and sedimentation* (Prentice Hall Inc. New Jersey), 430 pp.
- [11] Galvin, C.J. Eagleson, P.S.(1965). Experimental study of longshore current on a plane beach, (US Army Coastal Engineering Research Center, Washington D.C), 1965, pp.198. <https://apps.dtic.mil/sti/pdfs/ADA345211.pdf>